Monitoring the pozzolanic activity of fly ash in blended OPC mortars by electrical impedance spectroscopy

I.C. Fita[1], J.M. Cruz[1], N. Bouzón[2], M.V. Borrachero[2], J. Payá[2]

[1] Departamento de Física Aplicada, Universitat Politècnica de València, Camino de Vera s/n, 46022 Valencia, Spain.
[2] ICITECH, Instituto de Ciencia y Tecnología del Hormigón, Universitat Politècnica de València, Camino de Vera s/n, 46022 Valencia, Spain.
* corresponding author: Tel. 34 96 387 95 22, e-mail address: infifer@fis.upv.es

ABSTRACT

Fly ash (FA) is a pozzolanic material widely used to replace ordinary Portland cement (OPC) in mortars and concretes. The main purpose of this replacement is to reduce the consumed amount of cement, for economic and environmental reasons.

Main technical advantages, such as the improvement in durability and the enhancement of mechanical properties with long-time hydration, are derived from the pozzolanic activity. Several studies aimed to evaluate the pozzolanic reaction extent have been reported by using thermogravimetric analysis (TGA), mechanical compressive strength and mercury intrusion porosimetry (MIP). Besides, other complementary non-destructive techniques that reflect the effect of FA on microstructure are of great scientific and technical interest.

In this work, an alternative non-destructive method, the electrical impedance spectroscopy (EIS) followed by the equivalent circuit analysis (EC) has been applied to identify two electrical relaxations, which are strongly associated to microstructural properties.

The high frequency relaxation was assigned to the electrical conductivity of the calcium silicate hydrate (C-S-H) gel. Additionally, this C-S-H gel conductivity was separated into dc-conductivity and frequency-dependent conductivity, that provided information regarding the periods of early pozzolanic reaction (around 12 days) and high pozzolanic activity (around 28 days).

This research provides conclusive evidence of the validity of the applied EIS-EC method on account of the significative relationships found between electrical parameters and physicochemical properties determined by TGA, compressive strength and MIP.

Specifically, non-evaporable water, compressive strength and gel-pore-volume of diameter less than 10 nm exhibited significative exponential correlations with dc-electrical resistivity of the high frequency relaxation. These correlations validated the appropriate allocation of the high frequency relaxation to C-S-H gel.

Key words: Fly ash, mortar, C-S-H gel microstructure, electrical-impedance-spectroscopy, impedance-relaxation.

1. INTRODUCTION

Supplementary cementitious materials are widely used as a replacement for ordinary Portland cement (OPC) in cement-based products for both, economic and environmental reasons. Fly ash (FA) is a by-product from the coal-fired power stations that can be applied as substitute of cement. FA particles change microstructural properties of mortars, decreasing the mobility of ions and improving its durability [1], [2].

In OPC based materials, FA particles consume portlandite that results from cement hydration, incorporating new hydrates from the pozzolanic reaction. The physicochemical properties of these pozzolanic hydrates depend in a complex way on: i) percentage of FA replacement, ii) fineness of the pozzolanic particles (specific surface area), iii) chemical composition (type of FA), iv) water/binder ratio (w/b), v) curing age and vi) temperature [3], [4], [5]. The replacement of cement by FA enhances the cement hydration extent by the particle effect (filler effect), which involves two passive mechanisms: increasing the nominal water/cement ratio (dilution effect) and providing an extra-surface for the hydration

of cement particles (nucleation effect). The outcome of both effects is an increase in the rate of cement hydration. The specific effect of FA is the pozzolanic reaction, which produces new calcium silicate hydrates (C-S-H), from the dissolved portlandite (CH), that have a different composition and morphology from those formed in plain OPC materials [6], [7], [8], [9], [10].

Fly ash of type F (calcium content <10%) is broadly used. In cement pastes with moderate-high replacement by FA (30-50%) some important physicochemical properties and critical curing ages have been reported by different techniques:

1) Mercury intrusion porosimetry (MIP) provides two porosity parameters: volume of intruded mercury and critical pore-entry radius [11], [12], [13]. Pastes with 40% of FA replacement have greater intruded volume than plain cement pastes from 28 to 90 days. The pozzolanic reaction has a significant effect on the porosity between 28 and 60 days, but it slows thereafter [8].

2) Thermogravimetric analysis (TGA) provides data of pozzolanic reaction, based on the content of portlandite (CH), and non-evaporable water (W_n) in cement pastes [9], [11], [14], [15], [16]. Both processes, cement hydration and FA reaction, contribute to increase W_n, while the content of CH correlates positively with the cement hydration extent, and negatively with the pozzolanic reaction. In plain pastes, CH is about 25% (in weight) at the age of 100 days [17]. The pozzolanic reaction consumes CH by incorporating Ca^{2+} into new hydrates (portlandite fixation). This reaction begins when a threshold amount of CH has been produced. The reduction of CH content due to pozzolanic reaction starts on day 7 [9], [11].

3) Mechanical compressive strength reflects differences in the microstructure related to the percentage of cement replacement by FA [14], [18], [19], [20], [21]. FA replacement in the range 10-25% can exceed the compressive strength of plain cement pastes and mortars at 90 days.
4) Electrical impedance spectroscopy (EIS) is a non-destructive technique used to detect differences in the microstructure of pastes, mortars and concretes with FA replacement over time. Some studies have been done in the initial hours [22], [23], [24], [25], [26] and other studies at older ages [27], [28].

In recent decades, there have been a great interest in measuring electrical properties of OPC based materials. These measurements are based on applying low electrical current at different frequencies, aimed to estimate microstructural properties by a non-destructive method. First works were published by McCarter [29], [30].

The most common measuring procedure consists of three steps: i) the use of metal electrodes attached to the material ii) the measurement of impedance (EIS) or capacitance (Dielectric Spectroscopy) and iii) the search for an equivalent circuit (EC) with the same electrical response that the material. The EC is composed of discrete elements R and C, o distributed elements like constant phase element CPE, o Warburg impedance. Different EC have been used with electrical elements in parallel [27], [31], [32], [33], [34], [35], [36] in series [37], [38], [39], or even specific circuits with Warburg impedance such as the Randles circuit [40], [41].

OPC blended mortars are disordered microscopic mixtures of conductive and dielectric particles, randomly distributed with different microstructure or microgeometry. A good approach to improve the knowledge of disordered composites has been developed by the impedance analysis of two-dimension electrical networks, composed of a high number of purely resistive (R) and purely capacitive (C) elements randomly arranged, in different percentages [42], [43], [44]. The EC of these networks at different frequencies requires one or more distributed elements, that are characterized by a time constant (or characteristic frequency of relaxation) and a fractional exponent (ranged between 0 and 1). Hamou et al. [42] applied a high-resolution and accurate complex-nonlinear-least-squares fitting by using LEVM program [45], [46] to obtain the EC with distributed elements [44]. The main results of this research are: i) a good fitting of experimental data to an EC requires the use of two distributed elements corresponding to two relaxations, ii) time constant and fractional exponent that characterize each relaxation vary with the selected EC and iii) one of the fractional exponents is always around 0.5 which represents the percolation threshold in two-dimension systems composed by conductive and dielectric elements. Although time constant of each relaxation has not got any direct physical meaning, it is related to the percentages of conductive and dielectric elements.

Two relaxations are likewise found in our previous papers on electrical impedance for OPC mortars, with fractional exponents of 0.5 and 0.8, respectively [27], [39]. A decrease in exponent 0.8 by 37% is obtained after applying several cycles of drying-rewetting that reflects a change of microstructure in C-S-H gel, nevertheless exponent 0.5 barely changes [39]. Regarding the physical meaning of fractional exponents, the 0.8 exponent in hardened cement products is related with the fractal dimension of C-S-H gel [31], [47], [48], [49]. On the assumption that fractional exponent of 0.5 can be associated to the conductivity on surfaces [44], in OPC mortars it could be related to big pores.

As far as we know, few studies about high replacement by FA in blended mortars and long-time curing have been reported relating electrical parameters, deduced by EIS and EC, and physicochemical parameters, deduced by TGA, compressive strength and MIP.

In this work, we present an experimental study about hydration of OPC mortars blended with low-calcium fly ash, diameter of particle similar to the cement one, water/binder=0.5, during the period from 3 to 90 days, at ambient temperature (20 ± 1 ºC). The percentages of replacement of cement by FA were 0%-25%-40%-55%-70%.

The aim of this work is to study the effect of different FA percentages on the cement hydration and the pozzolanic reaction, through EIS measurements in the range of 100 Hz to 1 MHz and with the analysis of two relaxations by EC. Each relaxation was represented by a pair of elements in parallel (RQ). R represents the dc-resistance of bulk pore solution and Q is a constant phase element that represents the frequency-dependent conductance related to the surface or volume around the pore solution [27], [35], [38], [39]. The chosen EC was: $(R_LQ_L)(R_HQ_H)$, according to the circuit description code [50], that represents two relaxations, one of low frequency (LF) and another of high frequency (HF). Using the same EC allows to compare electrical properties between plain mortar and FA mortars.

Following this approach, this article investigates the cement hydration and FA pozzolanic reaction on the basis of EIS-EC. Critical ages related to the particle effect and the pozzolanic effect of FA, were deduced from the evolution of electrical parameters. In order to further test these results, electrical parameters were compared with those obtained by classical methods: TGA, compressive strength and MIP.

The section of results and discussion is organized as follows: firstly, impedance results as a function of frequency are shown and the values of the main parameters of the EC are presented; secondly, the evolution of the most significative electrical parameters of HF-relaxation is studied. Finally, a comparative analysis is performed between electrical resistivity of the HF-relaxation, obtained from the non-destructive EIS-EC method, and the physicochemical properties, CH, W_n, compressive strength and pore volume.

2. EXPERIMENTAL

2.1 Materials

Portland cement type CEM I-52.5R, with a mean particle diameter of 16.70 μm, was used as cementitious binder. Fly ash particles of type F (low CaO content) were milled to a mean diameter of 13.40 μm. Chemical compositions of cement and FA are shown in **Table 1**. Tap water was used to mix the raw materials into pastes and mortars. The aggregate used for mortars was of siliceous type, with a fineness modulus of 4.3.

Table 1
Chemical composition (% by weight) of cement and fly ash. Loss on ignition (L.O.I), mean particle diameter (D_m).

	SiO_2	Al_2O_3	Fe_2O_3	CaO	MgO	SO_3	K_2O	Na_2O	L.O.I	D_m (μm)
Cement	19.90	5.38	3.62	63.69	2.14	3.66	1.17	0.10	2.02	16.70
Fly ash	51.59	27.54	12.95	2.35	1.00	0.51	2.53	0.40	1.20	13.40

2.2 Preparation of cement pastes and mortars

Pastes and mortars were prepared according to UNE-EN-196-1:2005 [51] and UNE-EN 197-1:2011 [52] standards.

For cement pastes, cement and FA were first mixed in a sealed plastic container, then water was added and blended until a homogeneous mixture was obtained. The container was closed and kept in a humid chamber at a temperature of 20 ± 1 °C and RH > 90% (curing conditions), to the age selected for the measurements.

For mortars, water was poured into a 5-liter mixer, then a homogenized mixture of cement and FA was added and, finally, the aggregate. Molds of 40 x 40 x 160 mm^3 were filled as they were compacted. For the first 24 hours, the samples were kept under humid chamber conditions. After that time, they were demolded and immersed in saturated lime solution at a temperature of 20 ± 1 °C (curing conditions). Three samples of each mortar were prepared for electrical, physicochemical and mechanical measurements.

Nomenclature and dosage of cement pastes and mortars are shown in **Table 2**.

Table 2
Dosage of cement pastes (p0: plain cement paste, pX: blended pastes with X(%) of FA replacement), and mortars (m0: plain OPC mortar, mX: blended mortars with X(%) of FA replacement). X ratios calculated with respect to binder b in weight (b = cement + FA).

Label	Cement (c) (g)	Water (w) (g)	aggregate (agg) (g)	Fly ash (FA) (g)	Binder (b=c+FA) (g)	FA/b X (%)	w/b (-)	agg/b (-)
p0	450.0	225.0	-	0	450	0	0.50	-
p25	337.5	225.0	-	112.5	450	25	0.50	-
p40	270.0	225.0	-	180.0	450	40	0.50	-
p55	202.5	225.0	-	247.5	450	55	0.50	-
p70	135.0	225.0	-	315.0	450	70	0.50	-
m0	450.0	225.0	1350.0	0	450	0	0.50	3
m25	337.5	225.0	1350.0	112.5	450	25	0.50	3
m40	270.0	225.0	1350.0	180.0	450	40	0.50	3
m55	202.5	225.0	1350.0	247.5	450	55	0.50	3
m70	135.0	225.0	1350.0	315.0	450	70	0.50	3

2.3 Thermogravimetric analysis

This method consists of applying heat in the interval of 35-600 °C (at the rate of 10 °C / minute) in an inert atmosphere of dry N_2, and measuring the mass of the sample continuously. The amount of portlandite (CH(%)) and non-evaporable water (W_n(%)), both expressed as a percentage by weight of the sample, were determined from the loss of weight of the sample as temperature increased.

2.4 Mechanical compressive strength

The measurements were taken with an Instron Model 3382 universal machine. The test machine applied a speed of 2400 N/s, with an accuracy of 1%.

2.5 Mercury intrusion porosimetry

Porosity was determined using an AutoPore IV 9500 from Micrometrics Instrument Corporation with an intrusion pressure between 13782 Pa and 227.4 MPa (pore size between 5.5 nm and 361 μm). The samples were previously dried at 105 °C. Two parameters were measured: pore volume as a function of diameter, according to the Washburn relation, and total pore volume.

2.6 Electrical impedance spectroscopy

Electrical impedance measurements were taken with an HP-4284A impedance meter over the frequency range 100 Hz – 1 MHz. A constant current of 100 μA was applied in order to reduce and keep constant any electrochemical effect.
Fig. 1 shows a detailed picture of the measuring cell with a mortar sample connected to the impedance meter. The measuring cell consisted of two parallel gold-plated electrodes of 4 x 7 cm^2 separated by a

distance of 80 mm. A 4 x 4 x 16 cm^3 prismatic sample was placed in the cell, leaving two prismatic gaps of 2 x 4 x 7 cm^3 between the sample and the electrodes. These gaps were filled with the same lime saturated solution in which the mortar was conserved throughout the experiment. Impedance Z_m was measured at four different heights of the lime solution in the gap: h = 1.5, 3, 4.5 and 6 cm.

Electrical measurements were taken for three samples of each mortar at the curing ages: 3, 7, 12, 21, 28, 35, 56, 79 and 90 days. These measurements provided impedance data which include parasitic effects in series (cables and connectors), and in parallel (the edge of the prismatic sample at its lower and upper ends, and its side surface). The series-parasitic impedance was removed by subtracting the measured short-circuit impedance Z_{cc} from the measured impedance Z_m, and resulting in the corrected impedance Z_{co} ($Z_{co} = Z_m - Z_{cc}$) for each height. The parallel-parasitic admittance of lower and upper ends of sample (Y_{pa}) was removed by fitting data of Y_{co} (Z_{co}^{-1}) to the different measuring heights of solution (h): $Y_{co} = Y_h \cdot h + Y_{pa}$, for both, real and imaginary parts (variable area method). The impedance, proportional to height Z_h (Y_h^{-1}), is free of parasitic impedances except for the capacitive external admittance Y_c of the side surface. Impedance Z_h matches with the electrical resistivity which includes three impedances in series, $Z_h = Z_{mo} + Z_{es} + R_{sol}$, the intrinsic impedance of the mortar Z_{mo}, the corresponding to the interface electrodes-solution Z_{es}, and the resistance of the saturated solution R_{sol} that was measured independently. The free CNLS LEVM program [45], [46] was applied to Z_h by using an EC in order to separate the series impedance Z_{mo}, Z_{es} and Y_c in parallel (**Fig. 2 (e)**). Y_c is not shown in the EC.

For mortars, a relaxation is represented in EC by a pair of elements in parallel (RQ) [27], [39]. The inverse of resistance R represents the dc-conductivity, and Q is a constant phase element which represents the frequency dependent conductivity. The admittance Y_Q (Z_Q^{-1}) is defined as: $Y_Q = Y_0 \cdot (j\omega)^n$ with Y_0 and n being the characteristic parameters, j the unity of imaginary numbers and $\omega = 2 \cdot \pi \cdot$frequency. The characteristic frequency of the relaxation is calculated as:

$$f = [2\pi]^{-1}(RY_0)^{-\left(\frac{1}{n}\right)} \quad (1)$$

The exponent n indicates the relaxation shape in the Nyquist plot (imaginary part of Z versus real part of Z). If n = 1 the plot appears as a semicircle, but if n < 1 the plot is represented by a flattened semicircle.

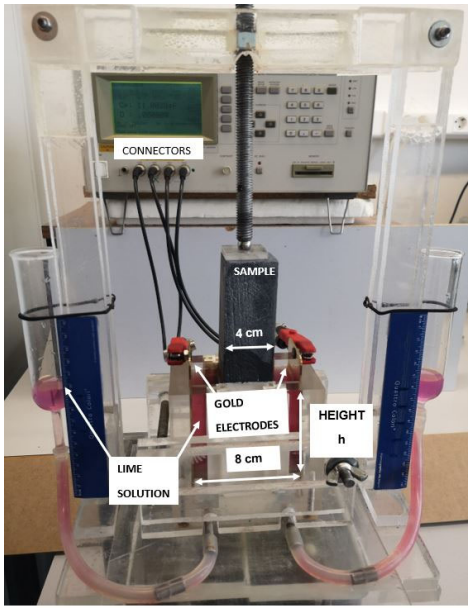

Fig. 1. Impedance meter and measuring cell

3. RESULTS AND DISCUSSION

3.1 Electrical parameters of the equivalent circuit

Fig. 2 shows Nyquist diagrams of the measured impedance (Z) (imaginary part Im(Z) as a function of real part Re(Z)) for one sample of each mortar, on days 3 (**Fig. 2 (a) and (b)**) and 90 (**Fig. 2 (c) and (d)**), as an example. Impedance plots exhibited a typical double branch with “V" shape which represents two impedances associated in series with two characteristic frequencies separated in the frequency domain. The branch of low frequency (on the right) corresponded to the electrode-solution interface. It had an imaginary part with values in the range of -0.5 to -1 Ω·m, without scarcely changes in the measurement period, which are unnoticeable in the graphs on day 90 for scale reasons. The medium-high frequency branch (on the left) reflects the mortar impedance. At the highest frequency of 1 MHz, the imaginary part reached low values in the range of -0.3 to -1.5 Ω·m on day 3, and greater values in the range of -5 to -90 Ω·m on day 90. Re(Z) and Im(Z) grew significantly over time for FA mortars in comparison with plain mortar.

At the frequency in which Im(Z) took the lowest absolute value, the real part of the impedance ranged from 12.0 to 21.0 Ω·m on day 3, and with greater values from 47 to 380 Ω·m on day 90. These values represent the bulk dc-resistivity of mortar, R_b. On day 3, R_b decreased with FA content but on day 90 it increased with FA content. Therefore, the evolution of R_b highlights the particle effect of FA at 3 days and the pozzolanic effect at 90 days.

The EC used in this work is shown in **Fig. 2 (e)**, $R_{sol}\,Q_e\,(R_LQ_L)\,(R_HQ_H)$, following the circuit description code [50]. The set $R_{sol}\,Q_e$ represents the electrode-solution interface. Mortar was represented by two elements in parallel (R Q) arranged in series, exhibiting two impedance relaxations: (R_LQ_L) in the range of kHz (Low frequency, LF-relaxation) and (R_HQ_H) in the range of MHz (High frequency, HF-relaxation). The bulk resistivity of mortar is $R_b = R_L+R_H$.

The characteristic parameters of constant phase elements Q_L and Q_H are Y_{oL}, n_L, Y_{oH} and n_H. Electrical parameters of the EC were obtained by applying the LEVM program with uncertainties less than 3%: R_L (<1.0%), Y_{0L} (<1.0%), n_L (<0.2%), R_H (<0.05%), Y_{0H} (<3.0%) and n_H (<0.2%). The statistical parameters were: PDRMS (root mean square values of estimated relative standard deviation of the fitting residuals) < $20\cdot10^{-3}$, SF (relative standard deviation of the fit residuals) < $15\cdot10^{-3}$ and Res/Mod (residuals with respect to the model) < 7%. Data met the Kramers-Kronig requirements as the residuals presented random scattering [53].

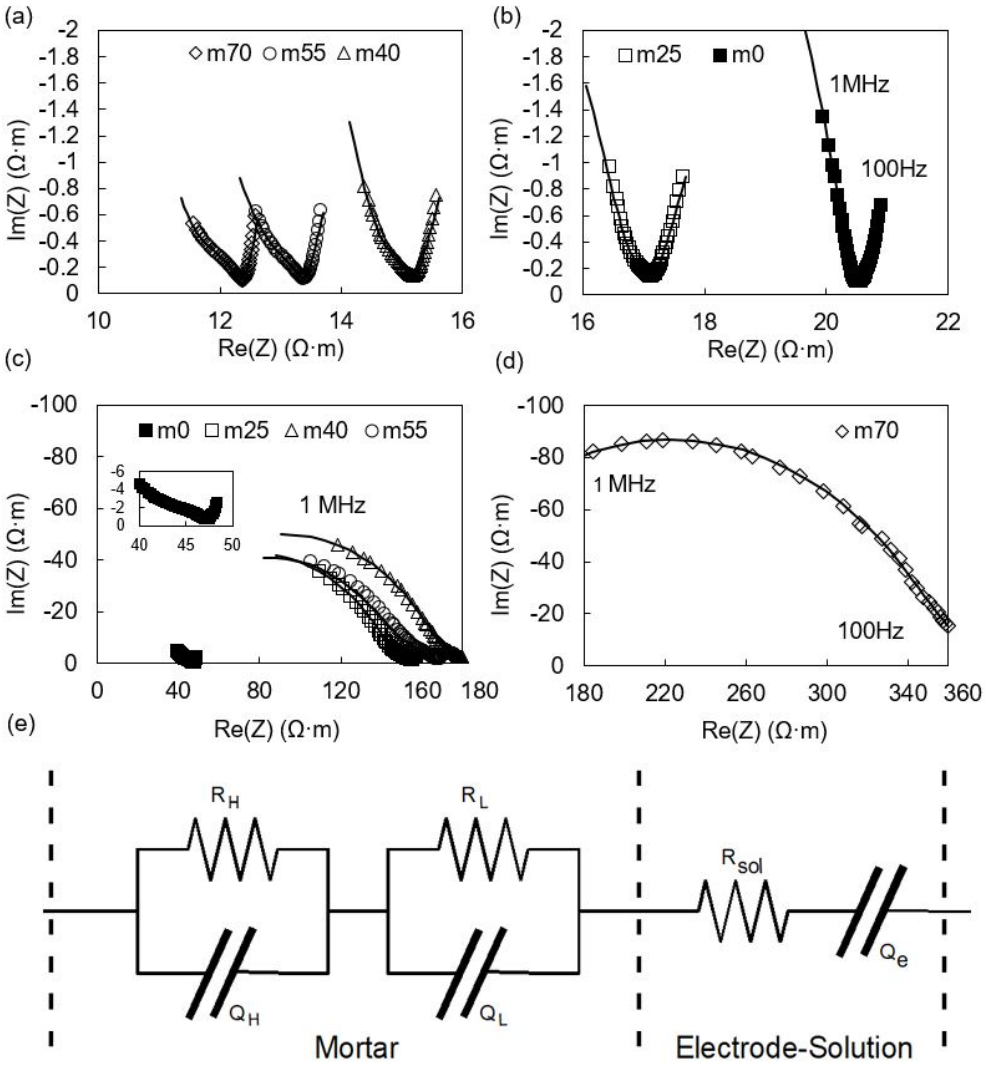

Fig. 2. Experimental Nyquist diagrams (imaginary part of Z vs real part of Z) and model fitting for: a) m40, m55, m70, and b) m25, m0 at 3 days, c) m0, m25, m40, m55 and d) m70 at 90 days. Inset: plain mortar m0. e) Equivalent circuit composed of: interface electrode-solution (R_{sol} Q_e) and mortar (R_LQ_L) (R_HQ_H). R_{sol} was a fixed and known value.

The main electrical parameters associated to HF and LF relaxations are summarized in **Table 3**. Resistances R_H and R_L represent the dc-electrical resistivity related to each relaxation as the measurement of impedance was corrected by the variable area method. Both resistivities determine the bulk resistivity, R_b (R_H+R_L), being the dc-resistivity of the percolated pore system of the sample. Resistivity R_H was about tens at early ages, it increased over time, doubling for plain mortar and reaching few hundreds for FA mortars at 90 days. Resistivity R_L was lower than R_H for all mortars in the whole period, starting with values less than the unit and reaching few tens at 90 days. In the period 3-28 days, the ratio between both resistivities was: R_H/R_L > 15 for m0 and R_H/R_L > 6 for m70, being this the lowest ratio of all FA mortars.

Fractional exponents n_H and n_L represent the capacitive feature of each relaxation. Exponent n_H ranged between 0.95 and 0.84 on day 3, and between 0.85 and 0.65 from day 7 on, decreasing with FA content. Exponent n_L ranged between 0.37 and 0.55, and the most frequent value was 0.5 ± 0.05. This common value around 0.5 for both plain mortar and FA mortars seems to be a microstructure feature common to all mortars, regardless of the binder used in the initial mixture.

Characteristic frequency f_x (x = H, L) was calculated with equation (1). The characteristic frequencies were about tens of MHz for HF-relaxation and tens of KHz for LF-relaxation (**Table 3**). These values and their corresponding time constants do not have physical meaning regarding the study of two-dimensions

electrical network of discrete elements R and C [44] but they confirm the presence of two different conductive spaces.

Table 3
Main electrical parameters of high (H) and low (L) frequency relaxations. R_H (Ω·m), n_H (-), f_H (MHz), R_L(Ω·m), n_L(-) and f_L(kHz) obtained as the mean of three samples with relative uncertainties less than 5%.

Time	3 days					7 days					12 days				
	m0	m25	m40	m55	m70	m0	m25	m40	m55	m70	m0	m25	m40	m55	m70
R_H	18.88	15.24	12.80	10.51	9.63	24.21	21.17	18.33	16.01	17.42	28,00	26.11	25.46	24.81	22.24
n_H	0.85	0.84	0.91	0.95	0.91	0.84	0.84	0.83	0.83	0.78	0.85	0.82	0.80	0.76	0.72
f_H	21.65	27.52	28.80	19.14	16.84	18.89	20.73	23.72	26.72	26.03	17.07	17.26	16.48	16.71	17.98
R_L	0.36	0.73	1.15	1.77	1.65	0.35	1.04	1.39	1.59	1.84	0.41	1.22	1.80	2.20	2.22
n_L	0.37	0.51	0.48	0.47	0.50	0.42	0.52	0.51	0.52	0.55	0.46	0.54	0.55	0.56	0.55
f_L	15.80	151.00	300.38	835.41	631.15	20.54	71.74	80.11	89.76	67.69	22.08	35.97	32.17	30.89	39.87

Time	21 days					28 days					35 days				
	m0	m25	m40	m55	m70	m0	m25	m40	m55	m70	m0	m25	m40	m55	m70
R_H	29.00	39.50	48.88	37.42	31.33	30.03	45.95	55.93	40.06	37.48	31.86	59.97	69.59	50.65	46.01
n_H	0.85	0.77	0.76	0.70	0.65	0.82	0.74	0.73	0.68	0.65	0.81	0.75	0.74	0.71	0.66
f_H	15.68	11.82	8.45	10.58	11.72	16.50	9.66	6.84	9.10	5.14	16.97	6.98	5.14	6.60	5.79
R_L	0.59	2.12	3.73	3.51	3.53	1.80	3.05	5.15	5.16	5.69	3.57	4.95	7.91	9.33	8.26
n_L	0.48	0.51	0.54	0.54	0.51	0.46	0.48	0.50	0.49	0.50	0.43	0.46	0.47	0.45	0.49
f_L	41.83	22.27	15.86	20.88	32.83	80.25	20.26	15.30	30.21	17.42	170.29	20.86	17.42	42.01	38.90

Time	44 days					56 days					90 days				
	m0	m25	m40	m55	m70	m0	m25	m40	m55	m70	m0	m25	m40	m55	m70
R_H	33.97	73.63	84.26	63.69	68.04	34.40	96.11	105.30	86.58	120.05	37.78	136.44	167.42	143.63	336.71
n_H	0.80	0.75	0.74	0.72	0.67	0.81	0.75	0.73	0.71	0.70	0.80	0.75	0.74	0.71	0.70
f_H	14.13	5.19	3.93	4.67	3.54	15.15	3.80	2.90	3.23	1.79	16.02	2.76	1.96	1.94	0.57
R_L	3.61	7.89	10.42	15.23	12.57	5.09	10.90	12.67	13.87	15.32	10.58	16.37	16.74	20.11	26.94
n_L	0.49	0.42	0.46	0.44	0.49	0.54	0.43	0.47	0.49	0.53	0.50	0.45	0.51	0.50	0.55
f_L	287.64	24.68	15.76	47.30	25.61	116.76	19.38	10.75	16.69	6.94	36.19	31.68	5.23	7.86	1.51

Since R_L was much lower than R_H and n_L is around 0.5 for all mortars, resistivity R_L and n_L must be associated to larger pores located out of the gel space whose pores are in the nanometric scale. Therefore, it is reasonable to assume that R_H, n_H and f_H are related to the C-S-H gel, both in plain mortar and FA mortars [47], [48], [49].

In the next two subsections, the evolutions of resistivity R_H and exponent n_H over time are presented to monitor cement hydration and pozzolanic reaction, then, a comparative study between R_H and physicochemical properties deduced from TGA, compressive strength and MIP is developed to validate the relationship between the HF-relaxation and C-S-H gel described previously.

3.2 Evolution of electrical parameters of HF-relaxation

Fig. 3 shows the temporal evolution of the conductivity S_H (mS/m), calculated as the inverse of the resistivity $S_H=(R_H)^{-1}$ in mS/m and represented in log-log scale. Good linear regressions were carried out for $\log(S_H/S_r)$ vs $\log(time/time_r)$, with determination coefficients higher than 0.94. Coefficients S_r and $time_r$ being reference conductivity (1 mS/m) and reference time (1 day), respectively. Every mortar exhibited two linear relationships, one from 3 to 28 days and another from 35 to 90 days. The logarithmic decreasing of S_H followed the logarithmic evolution of cement and pozzolanic hydrations [16], [49].

Conductivity was positively correlated with the percentage of replacement on day 3, then S_H decreased continuously over time, reaching the lowest values and being inversely correlated with FA content on day 90.

Two linear equations were obtained for plain mortar, the first from 3 to 28 days, and the second from 35 to 90 days, both following the rate of cement hydration. The first slope was -0.21 and the second -0.18, showing a slower rate of cement hydration after day 28.

Also, two linear equations were obtained for FA mortars with slopes higher than m0, for the same two periods. In the first period 3-28 days, FA mortars presented higher rates of change than m0 (-0.50, -0.69, -0.63 and -0.60 for m25, m40, m55 and m70, respectively). These higher slopes reflected the acceleration of cement hydration rate via the particle effect (dilution and extra surface for hydration). Mortar m40 was found to be the one with the highest slope (-0.69) in this period, due to an appropriate cement/FA ratio (60% of cement content and 40% of FA content), that produced a positive synergy between cement hydration and particle effect of FA.

In the second period 35-90 days, slopes experienced a significant growth with values of -0.87, -0.9, -1.13, -2.18 in the increasing order of FA replacement. These rates, much greater than -0.18 for plain mortar, reflected the formation of new hydrates on account of a high pozzolanic activity.

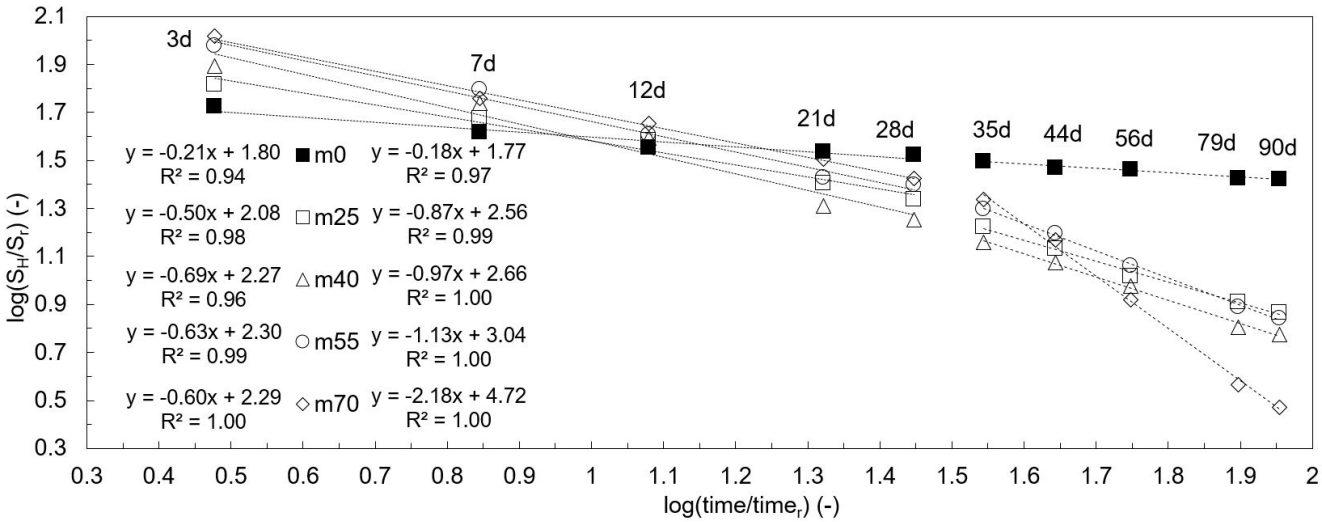

Fig. 3. Log-log plot of S_H/S_r vs time/time$_r$ between 3 and 90 days for all mortars. S_r and time$_r$ being reference conductivity (1 mS/m) and reference time (1 day), respectively. The fittings were calculated for two periods: 3-28 days (left) and 35-90 days (right). Linear regressions presented determination coefficients (R^2) higher than 0.94.

In order to better observe the relative effect of FA over time, conductivity of each FA mortar was normalized with respect to plain mortar S_H/S_{H0} (**Fig. 4**). The normalized conductivity was greater than the unit, and it was positively correlated with the amount of FA in the period 3-12 days.

This relative parameter indicates the positive overall effect of FA on conductivity in the first two weeks, as a result of the dilution effect (more water per cement unit), that exceeded the nucleation effect (greater hydration surface in FA particles). Therefore, in the first 12 days, FA mortars had more free water, which resulted in higher conductivities than that for plain mortar. Between 12 and 28 days, conductivity changed in all FA mortars from being above to being below the one for plain mortar.

From day 28 on, the relative conductivity experienced a continued decline, reaching percentages ranging from 10% to 30% at 90 days. Mortar m70 had the highest value until day 35, but the lowest value from 56 days on, indicating the greatest relative change in S_H between 35 and 56 days. Since conductivity S_H is related to the total hydrates derived from cement hydration and pozzolanic reaction, it is a simultaneous and continuous process and therefore it cannot exactly reflect the beginning of pozzolanic activity.

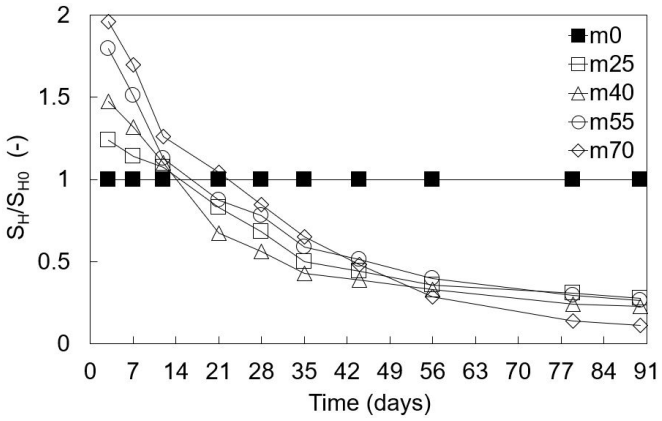

Fig. 4. Normalized dc-electrical conductivity of HF-relaxation in mortars with respect to the plain mortar (S_H/S_{H0}) between 3 and 90 days of curing age.

In order to determine the beginning of pozzolanic reaction the capacitive exponent n_H was analyzed. **Fig. 5** depicts the capacitive exponent n_H for all mortars. This parameter characterizes the electrical conductivity on the surface of the percolated pore structure of the C-S-H gel [35], [48], [49]. Variations of n_H indicate changes or differences in the microstructure of C-S-H gel [39].

Plain mortar displayed values between 0.85 and 0.80 at 3-7-12 days and around 0.80 from 21 days on, showing a stable microstructure of C-S-H gel. However, exponent n_H of FA mortars varied with respect to m0 one. In the first week, it was higher than that of m0, m55 being the highest on day 3, followed by m40 and m70. At 12 days, n_H was below than that of m0 for all FA mortars. Exponent n_H reached the lowest value between 0.75 and 0.65, in the increasing order of FA content, around day 28. Therefore, this decrease in n_H for FA mortars reflected the formation of a new fractal structure on the surface of the solid phase of the gel associated to the pozzolanic activity. At later ages, from 79 to 90 days, n_H increased around 0.70 and 0.75, that indicated a stable and similar microstructure among FA mortars, with new hydrates derived from the pozzolanic reaction, but quite different from the microstructure of cement hydrates [8], [17].

The joint analysis of the two parameters S_H and n_H showed the impact of FA on ionic conductivity, in the pore solution of the C-S-H gel and in the interface between this solution and the solid surface, respectively. These electrical parameters not only reflected the quantitative and qualitative variation of conductivity but also did manifest the evolution of pozzolanic reaction. Considering these changes, three periods of pozzolanic activity were identified for FA mortars: 1) an activation period, around 12 days, time in which S_H for FA mortars decreased to similar values to that for plain mortar and n_H became smaller than that for plain mortar; 2) high activity period, around 28 days, from which the rate of change of S_H increased (change of slope) and the lowest value of n_H was achieved; 3) a stable activity period, from 35 to 90 days with a continuous decrease of S_H but with an increase in n_H to asymptotic values.

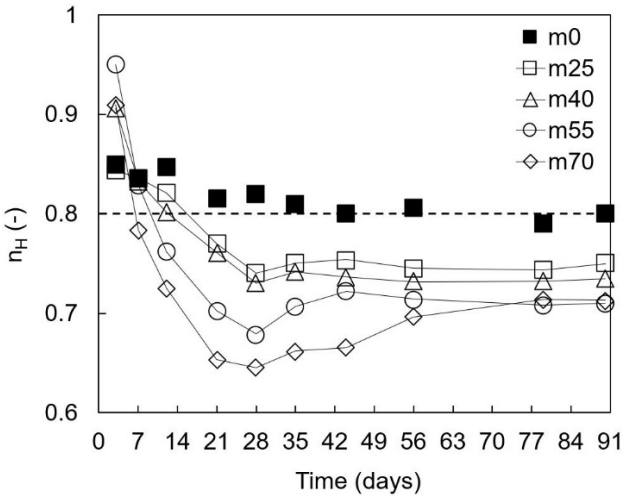

Fig. 5. Exponent of the HF-relaxation n_H for all mortars between 3 and 90 days of curing. The dashed horizontal line in 0.80 is drawn as an eye reference.

3.3 Comparative analysis. Electrical vs physicochemical parameters

Relative difference of portlandite in FA pastes with respect to the plain cement paste, (CH(%)) is defined as:

$$CH(\%) = \left[\frac{CH_x/CX(\%)-CH_0/100}{CH_0/100}\right]\cdot 100 \qquad (2)$$

CH_x and CH_0 being the portlandite content of FA paste with X(%) of FA replacement in paste pX and plain cement paste p0, respectively. CX(%) is the percentage of cement and X(%) is the percentage of FA replacement (CX(%)+X(%)=100).

CH(%) is zero for p0, while CH(%) is higher or lower than zero when CH_x, corrected by the percentage of cement, is more or less than the portlandite content for plain cement paste, respectively.

The relative difference of portlandite CH(%) is directly proportional to cement hydration, which produces CH, and inversely proportional to the pozzolanic reaction of FA, which consumes it. **Fig. 6 (a)** provides a bar chart of CH(%) for FA pastes at 7, 28, 56 and 90 days of curing.

On day 7, FA pastes had higher CH content than they would have had without the presence of FA (CH(%) > 0). Therefore, in the first week there was a positive effect of FA on cement hydration due to the particle effect. On the contrary, CH(%) was negative at 28, 56 and 90 days (except p25 on day 28) highlighting the high activity of pozzolanic reaction, which began before 28 days. The reduction of CH(%) was positively correlated with the FA content, and as a result, p70 was the only paste that consumed all the CH on day 90 (CH(%) = -100).

It is observed a formal similarity between S_H/S_{H0} and CH(%) represented in **Fig. 4** and **Fig. 6 (a)**, respectively. To quantify this similar behavior, S_H/S_{H0} of FA mortars was compared with the normalized content of portlandite CH_x/CH_0 of FA pastes, calculated from equation (2) as: $CH_x/CH_0=CX/100\cdot(1+CH(\%)/100)$. **Fig. 6 (b)** provides plots of S_H/S_{H0} for FA mortars vs CH_x/CH_0 of the corresponding FA pastes. According to **Fig. 6 (b)**, there was a positive and exponential correlation between both parameters for all mortars in the period 28-56-90 days. Determination coefficients were higher than 0.92. Pre-exponential coefficients were characteristic for every blended material, with values of 0.01, 0.04, 0.07, 0.12 in the increasing order of FA replacement.

Data on day 7 did not fit to the same function as the other three curing ages, due to the low pozzolanic activity in the first week [9], [11], [15]. Therefore, in the period from 28 to 90 days, the relative electrical conductivity of the HF-relaxation was a representative parameter of the pozzolanic reaction. This result proves that the consumed portlandite was fixed in new hydrates which formed a narrower pore network, responsible of the decrease in dc-conductivity of gel C-S-H, associated to HF-relaxation.

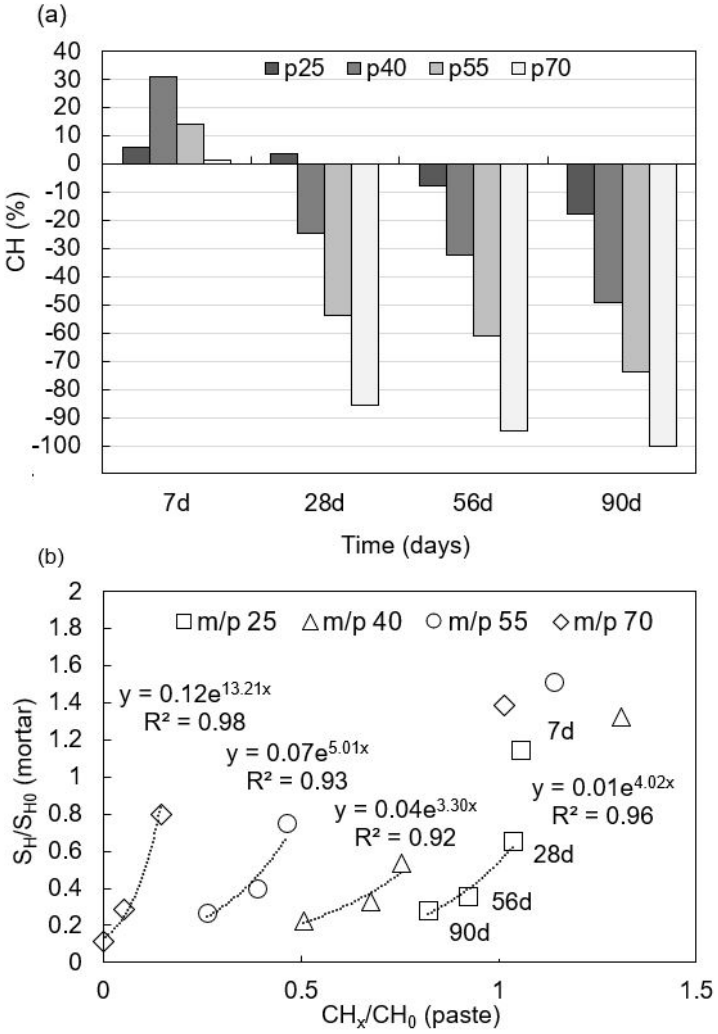

Fig. 6. (a) Relative difference of portlandite in FA pastes with respect to a plain paste. (b) Normalized conductivity in mortars with 25%, 40%, 55%, 70% of FA replacement as a function of normalized portlandite content in FA pastes with the same replacement. Exponential equations are shown, all determination coefficients being higher than 0.92 in the period 28-56-90 days.

Non-evaporable water W_n(%), associated with hydrated products derived from the hydration of cement and pozzolanic reaction of FA for cement pastes, is displayed in **Fig. 7 (a)**. The highest content of W_n(%) corresponded to plain paste p0, every day throughout the experiment. Non-evaporable water W_n(%) decreased with the percentage of replacement of cement by FA every measuring day [16].

Non-evaporable water W_n(%) increased continuously over time for all pastes, between 7 and 56 days for plain paste, and the whole period for FA pastes. The evolution of W_n(%) in the period 56-90 days for FA pastes shows that pozzolanic reaction was still active, increasing the amount of new hydrates to a larger extent.

Since the increase in dc-electrical resistivity is related to the content of hydrates, as they were responsible of the narrowing of the pore space, in **Fig. 7 (b)** R_H was represented as a function of W_n(%) measured in pastes with the same FA replacement.

Positive correlations between R_H and W_n(%) were found for all replacements, at the four ages of measurement. Exponential relationships between R_H and W_n(%) yielded reasonable correlations with determination coefficients higher than 0.97 for all mortars. Pre-exponential factor and the exponent were 2.41 and 0.15 for m0, and in the ranges 0.13-0.33 and 0.41-0.55 for FA mortars, respectively. Both parameters increased with FA replacement. Therefore, exponential model clearly distinguished plain mortar from FA mortars, and among FA mortars. This result accounts for the pozzolanic effect on R_H for

FA mortars. As would be expected, an increase in W_n(%) reflected the formation of new hydrates that reduced the porous space into C-S-H gel and it yielded an increase in the electrical resistivity.

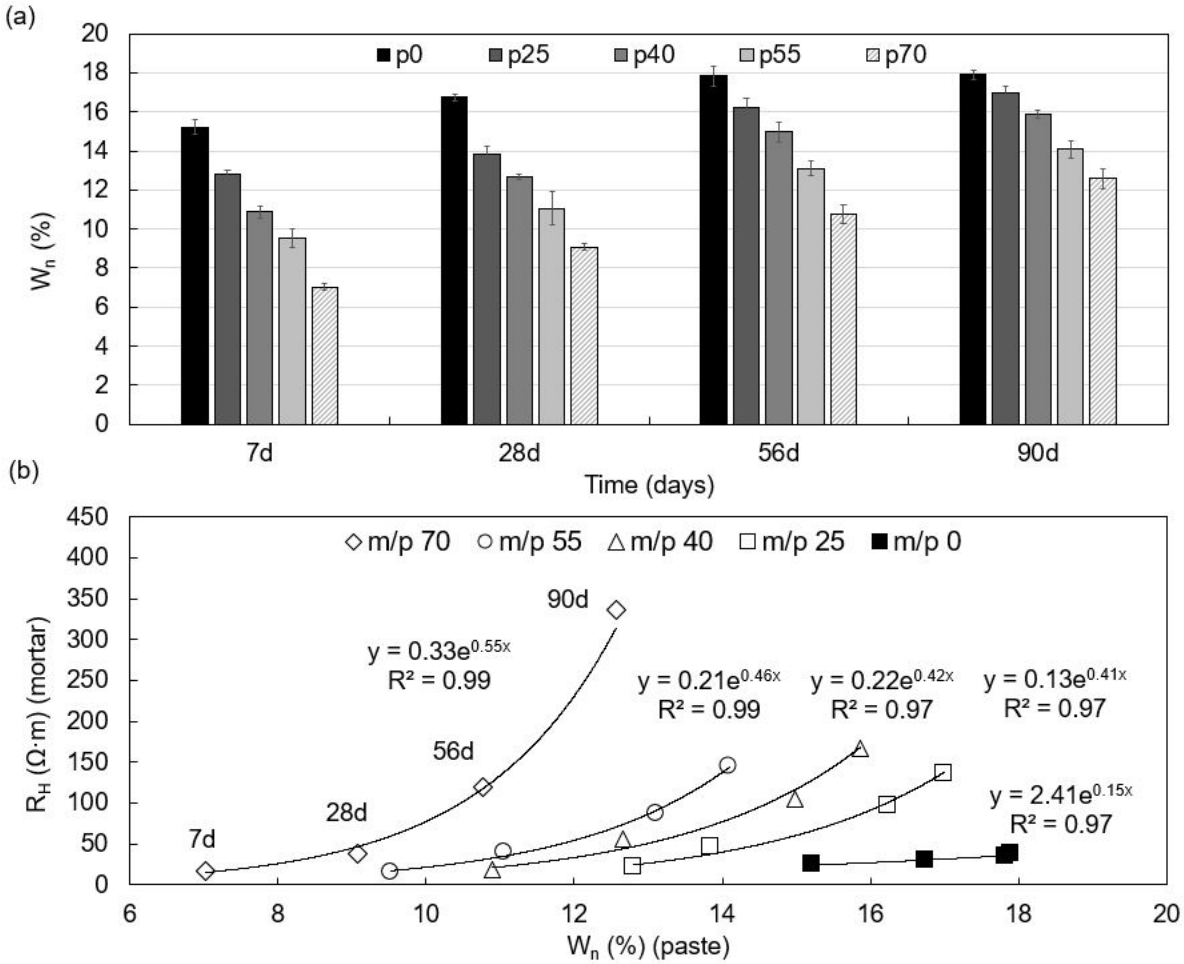

Fig. 7. (a) W_n(%) for all pastes at 7, 28, 56 and 90 days, (b) relationship between R_H of mortars and W_n(%) of the corresponding pastes. Exponential equations are shown with determination coefficients higher than 0.97. Error bars calculated for three samples.

Fig. 8 (a) shows compressive strength for all mortars on days 7-28-56-90. The value exhibited by m0, between 50 and 69 MPa, was higher than that for FA mortars in the whole period. Nevertheless, differences in compressive strength between m0 and FA mortars decreased over time, being around 10-20-30-40 MPa on day 7 and 3-5-15-30 MPa on day 90, for m25, m40, m55 and m70, respectively.

The estimation of compressive strength by a non-destructive method is considered of a great practical relevance, thus an analysis of the relationship between compressive strength and electrical parameters was performed. In **Fig. 8 (b)** the relationship between R_H and compressive strength for all mortars is shown. A positive correlation between both parameters was found. Exponential regressions were carried out for all mortars, with determination coefficients higher than 0.97 for all fittings. Similar relationships have been reported between compressive strength and the gel volume [14].

Pre-exponential factor was 8.61 (Ω·m) for plain mortar and 1.43, 2.34, 3.45 and 7.36 (Ω·m) for FA mortars in the increasing order of FA replacement (25%, 40%, 55% and 70%). Furthermore, it is interesting to note that the exponent of these equations was 0.02 for m0, 0.07 for m25, m40 and m55 for the entire period, and 0.09 for m70, indicating a similar microstructure of the matrix for m25, m40, m55 and a great difference between this group, m0 and m70. These exponential correlations reveal different mechanical

behavior of their microstructure, and clearly distinguish m0 and FA mortars, and even among FA mortars [14], [21].

For m70, the exponential function was obtained in the period 7-56 days, because at 90 days there was a high increase in R_H that did not have a correspondence with the low increase in compressive strength. Nevertheless, resistivity R_H was related to W_n(%) with an exponential correlation until 90 days, therefore we can infer that the hydrates formed at 90 days, with a lack of CH, did not contribute in the same way to the mechanical resistance as the hydrates formed at previous ages did.

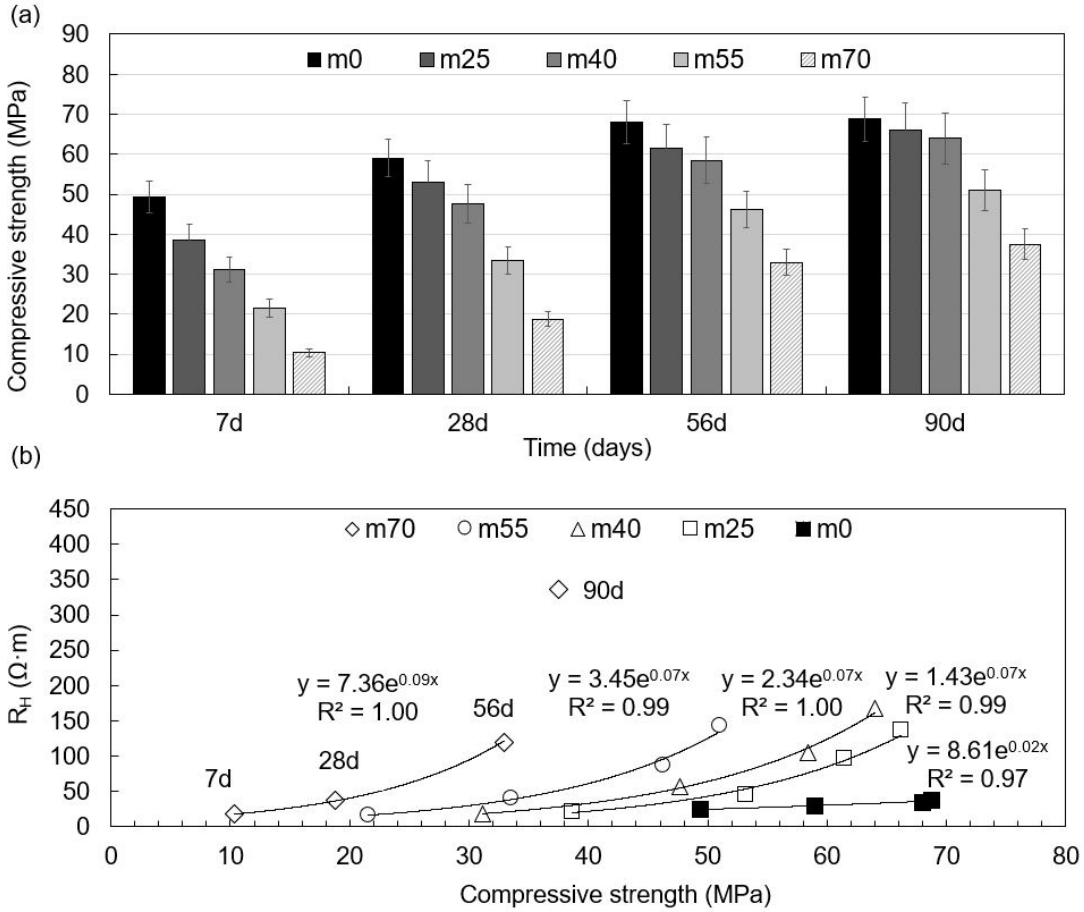

Fig. 8. (a) Compressive strength and (b) relationship between R_H and compressive strength for mortars at 1-28-56-90 days of curing. Exponential equations are shown with determination coefficients higher than 0.97. Error bars calculated for three samples.

Pore volume measured by MIP is represented as a function of pore diameter distribution for all mortars at 28 and 90 days of curing, **Fig. 9 (a)** and **(b)**.

The largest volume corresponded to the diameter range 10 nm-100 nm at the two ages, with values between 55% and 62% at 28 days and between 52% and 64% at 90 days. This pore volume changed from 28 to 90 days but it did not show any correlation with the FA content.

The pore volume associated to pores less than 10 nm was the second in magnitude. At 28 days, values were 10% for m0 and about 20% for FA mortars, but at 90 days, the pore volume decreased for all of them, exhibiting greater values in the increasing order of FA content.

On the assumption that smaller sized pores are those that have the greatest influence in the electrical resistivity R_H, in **Fig. 9 (c)** and **(d)** the relationship between R_H and pore volume of pores less than 10 nm was displayed at 28 and 90 days, respectively.

Comparing both days, R_H for FA mortars increased as the pore volume of diameter less than 10 nm decreased. The lowest values of R_H and pore volume corresponded to m0, at both ages. The highest values corresponded to m40 at 28 days and to m70 at 90 days. Between these extreme values the other FA mortars presented similar and intermediate values of R_H and pore volume.

The positive correlation between R_H and pore volume presented a good fitting to an exponential function, with acceptable determination coefficient of 0.89, at both ages. These good correlations validate the allocation of R_H to the C-S-H gel. Pre-exponential coefficient was similar at both ages, but the exponential coefficient considerably increased at 90 days. Therefore, on day 90, any increase in the pore volume yielded a higher change in the electrical resistivity than on day 28. This performance confirmed the differences between the microstructure for FA mortars at 28 and 90 days. These microstructures were mainly the result from cement hydration until 28 days and from two consecutive hydrations, cement hydration and pozzolanic reaction of FA until 90 days.

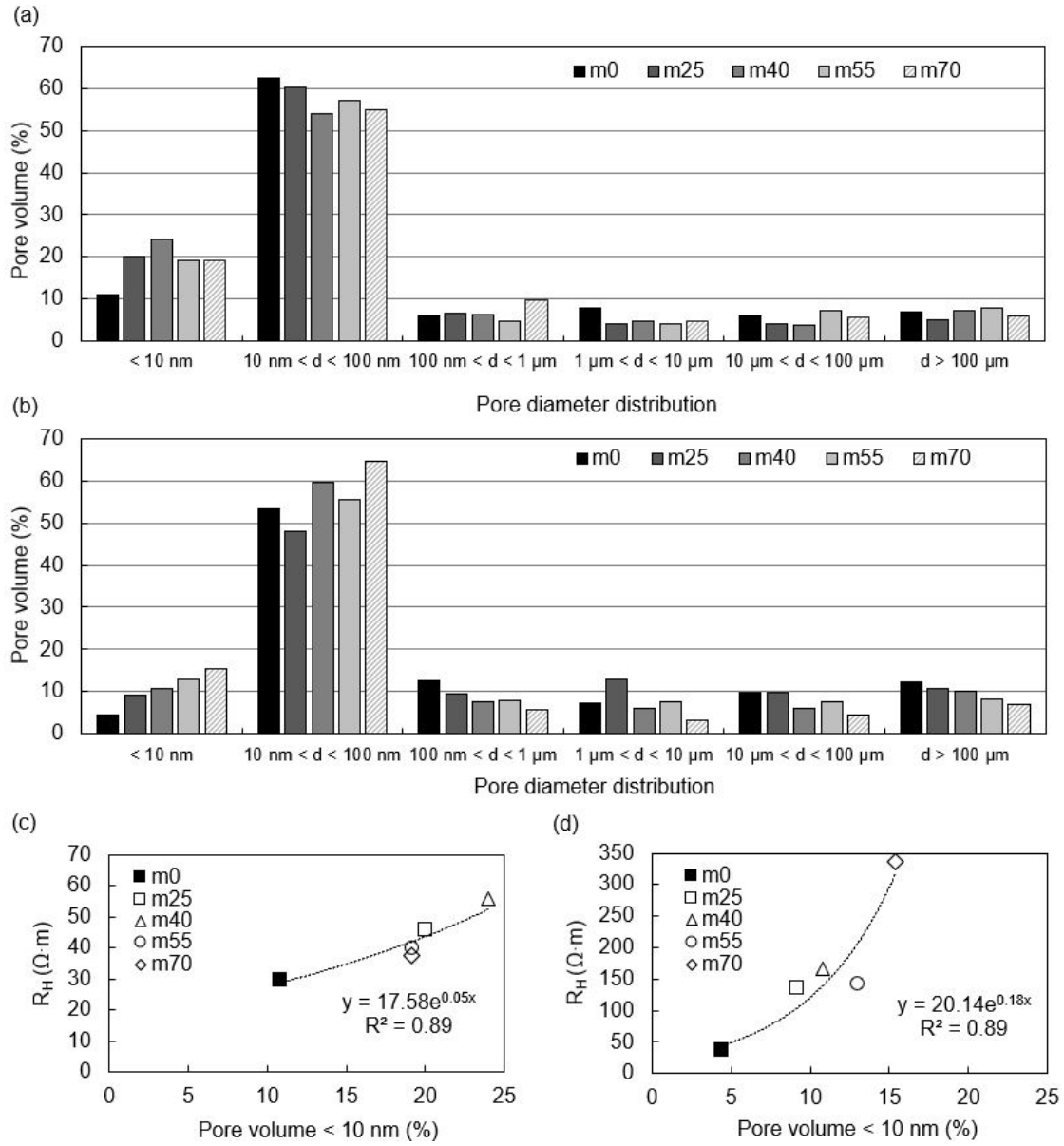

Fig. 9. Pore volume (%) distribution in different pore diameter ranges provided by MIP at (a) 28 days, (b) 90 days. Relationship between R_H and pore volume in pores of diameter < 10 nm at (c) 28 days (d) 90 days. Exponential equations are shown with determination coefficients of 0.89.

4. CONCLUSIONS

1) An analysis of the mortar impedance based on equivalent circuit allowed to identify two main relaxations: one in the high frequency (MHz) and another in the low frequency (kHz). The electrical conductivity related to the HF-relaxation was associated to nanopores of the C-S-H gel.

2) Dc-electrical conductivity of the HF-relaxation had a significative logarithmic relationship with time, reflecting two hydration periods, that were related with a main reaction, the cement hydration (3-28 days) and the pozzolanic hydration (35-90 days).

3) Dc-electrical conductivity of the HF-relaxation, for FA mortars, decreased continuously over time. It was higher than for plain mortar until the age of 12 days because of the dilution effect, and after that date, conductivity was lower than that for plain mortar, on account of the nucleation effect until 28 days and pozzolanic reaction from 28 days on. This fact involves a reduction of mobility of ions in the gel matrix of FA mortars, which has a direct effect on their durability.

4) Exponent of the HF-relaxation, that characterizes the frequency-dependent conductivity, barely changed in plain mortar but it decreased in FA mortars. This behavior reflected changes on the surface of C-S-H gel, allowing the monitoring of pozzolanic activity, with an activation period around 12 days and a peak of pozzolanic reaction around 28 days.

5) A good correlation with exponential regressions between dc-resistivity of the HF-relaxation and TGA parameters, portlandite content and non-evaporable water, proved the relationship between the increase in dc-resistivity of gel pore space and the content of hydrates.

6) Exponential function obtained between dc-resistivity of the HF-relaxation and compressive strength confirmed the correlation between the HF-relaxation and microstructural properties of the C-S-H gel, which could be used to predict compressive strength from non-destructive measurements of electrical impedance.

7) A positive correlation between dc-resistivity and the pore volume of pores less than 10 nm in diameter definitively validated the assignment of dc-resistivity of the HF-relaxation to the gel porosity in the nanometric scale.

REFERENCES

[1] M. Thomas, Optimizing the use of fly ash in concrete, (2007). https://www.researchgate.net/profile/Prem_Baboo/post/Is_Fly_ash_free_Blast_furnace_cement_or_Fly_Ash_Cement_better/attachment/59d6241679197b80779826bf/AS:310916627795968@1451139708741/download/is548-optimizing-the-use-of-fly-ash-concrete.pdf (accessed March 20, 2019).

[2] D.P. Bentz, C.F. Ferraris, K.A. Snyder, Best Practices Guide for High-Volume Fly Ash Concretes: Assuring Properties and Performance, (n.d.). doi:10.6028/NIST.TN.1812.

[3] S. Hanehara, F. Tomosawa, M. Kobayakawa, K. Hwang, Effects of water/powder ratio, mixing ratio of fly ash, and curing temperature on pozzolanic reaction of fly ash in cement paste, Cem. Concr. Res. 31 (2001) 31–39. doi:10.1016/S0008-8846(00)00441-5.

[4] P. Chindaprasirt, C. Jaturapitakkul, T. Sinsiri, Effect of fly ash fineness on microstructure of blended cement paste, Constr. Build. Mater. 21 (2007) 1534–1541. doi:10.1016/J.CONBUILDMAT.2005.12.024.

[5] M. Ben Haha, K. De Weerdt, B. Lothenbach, Quantification of the degree of reaction of fly ash, Cem. Concr. Res. 40 (2010) 1620–1629. doi:10.1016/J.CEMCONRES.2010.07.004.

[6] K. Luke, E. Lachowski, Internal Composition of 20-Year-Old Fly Ash and Slag-Blended Ordinary Portland Cement Pastes, J. Am. Ceram. Soc. 91 (2008) 4084–4092. doi:10.1111/j.1551-2916.2008.02783.x.

[7] B. Lothenbach, K. Scrivener, R.D. Hooton, Supplementary cementitious materials, Cem. Concr. Res. 41 (2011) 1244–1256. doi:10.1016/J.CEMCONRES.2010.12.001.

[8] E. Berodier, K. Scrivener, Evolution of pore structure in blended systems, Cem. Concr. Res. 73 (2015) 25–35. doi:10.1016/J.CEMCONRES.2015.02.025.

[9] F. Deschner, F. Winnefeld, B. Lothenbach, S. Seufert, P. Schwesig, S. Dittrich, F. Goetz-Neunhoeffer, J. Neubauer, Hydration of Portland cement with high replacement by siliceous fly ash, Cem. Concr. Res. 42 (2012) 1389–1400. doi:10.1016/J.CEMCONRES.2012.06.009.

[10] A.M. Rashad, A brief on high-volume Class F fly ash as cement replacement – A guide for Civil Engineer, Int. J. Sustain. Built Environ. 4 (2015) 278–306. doi:10.1016/J.IJSBE.2015.10.002.

[11] E. Sakai, S. Miyahara, S. Ohsawa, S.-H. Lee, M. Daimon, Hydration of fly ash cement, Cem. Concr. Res. 35 (2005) 1135–1140. doi:10.1016/J.CEMCONRES.2004.09.008.

[12] S. Ouellet, B. Bussière, M. Aubertin, M. Benzaazoua, Microstructural evolution of cemented paste backfill: Mercury intrusion porosimetry test results, Cem. Concr. Res. 37 (2007) 1654–1665. doi:10.1016/J.CEMCONRES.2007.08.016.

[13] Q. Zeng, K. Li, T. Fen-chong, P. Dangla, Pore structure characterization of cement pastes blended with high-volume fly-ash, Cem. Concr. Res. 42 (2012) 194–204. doi:10.1016/J.CEMCONRES.2011.09.012.

[14] L. Lam, Y.. Wong, C.. Poon, Degree of hydration and gel/space ratio of high-volume fly ash/cement systems, Cem. Concr. Res. 30 (2000) 747–756. doi:10.1016/S0008-8846(00)00213-1.

[15] Q. Zeng, K. Li, T. Fen-Chong, P. Dangla, Determination of cement hydration and pozzolanic reaction extents for fly-ash cement pastes, Constr. Build. Mater. 27 (2012) 560–569. doi:10.1016/j.conbuildmat.2011.07.007.

[16] Y.M. Zhang, W. Sun, H.D. Yan, Hydration of high-volume fly ash cement pastes, Cem. Concr. Compos. 22 (2000) 445–452. doi:10.1016/S0958-9465(00)00044-5.

[17] A. Cuesta, J.D. Zea-Garcia, D. Londono-Zuluaga, A.G. De la Torre, I. Santacruz, O. Vallcorba, M. Dapiaggi, S.G. Sanfélix, M.A.G. Aranda, Multiscale understanding of tricalcium silicate hydration reactions, Sci. Rep. 8 (2018) 8544. doi:10.1038/s41598-018-26943-y.

[18] C.S. Poon, L. Lam, Y.L. Wong, A study on high strength concrete prepared with large volumes of low calcium fly ash, Cem. Concr. Res. 30 (2000) 447–455. doi:10.1016/S0008-8846(99)00271-9.

[19] A. Oner, S. Akyuz, R. Yildiz, An experimental study on strength development of concrete containing fly ash and optimum usage of fly ash in concrete, Cem. Concr. Res. 35 (2005) 1165–1171. doi:10.1016/J.CEMCONRES.2004.09.031.

[20] M. Gesoğlu, E. Güneyisi, E. Özbay, Properties of self-compacting concretes made with binary, ternary, and quaternary cementitious blends of fly ash, blast furnace slag, and silica fume, Constr. Build. Mater. 23 (2009) 1847–1854. doi:10.1016/j.conbuildmat.2008.09.015.

[21] X.Y. Wang, K.B. Park, Analysis of compressive strength development of concrete containing high volume fly ash, Constr. Build. Mater. 98 (2015) 810–819. doi:10.1016/j.conbuildmat.2015.08.099.

[22] W.J. McCarter, G. Starrs, T.M. Chrisp, Immittance spectra for Portland cement/fly ash-based binders during early hydration, Cem. Concr. Res. 29 (1999) 377–387. doi:10.1016/S0008-8846(98)00209-9.
[23] W.J. McCarter, G. Starrs, T.M. Chrisp, The complex impedance response of fly-ash cements revisited, Cem. Concr. Res. 34 (2004) 1837–1843. doi:10.1016/j.cemconres.2004.01.013 ER.
[24] X. Wei, Z. Li, Study on hydration of Portland cement with fly ash using electrical measurement, Mater. Struct. 38 (2005) 411–417. doi:10.1007/BF02479309.
[25] S.W. Tang, X.H. Cai, Z. He, H.Y. Shao, Z.J. Li, E. Chen, Hydration process of fly ash blended cement pastes by impedance measurement, Constr. Build. Mater. 113 (2016) 939–950. doi:10.1016/J.CONBUILDMAT.2016.03.141.
[26] A. Husain, K. Kupwade-Patil, A.F. Al-Aibani, M.F. Abdulsalam, In situ electrochemical impedance characterization of cement paste with volcanic ash to examine early stage of hydration, Constr. Build. Mater. 133 (2017) 107–117. doi:10.1016/j.conbuildmat.2016.12.054.
[27] J.M. Cruz, I.C. Fita, L. Soriano, J. Payá, M.V. Borrachero, The use of electrical impedance spectroscopy for monitoring the hydration products of Portland cement mortars with high percentage of pozzolans, Cem. Concr. Res. 50 (2013) 51–61. doi:10.1016/J.CEMCONRES.2013.03.019.
[28] B. Suryanto, W.J. McCarter, G. Starrs, T.M. Chrisp, Characterization of Fly-ash using Electrochemical Impedance Spectroscopy, Procedia Eng. 171 (2017) 705–714. doi:10.1016/J.PROENG.2017.01.414.
[29] W.J. McCarter, S. Garvin, N. Bouzid, Impedance measurements on cement paste, J. Mater. Sci. Lett. 7 (1988) 1056–1057. doi:10.1007/BF00720825.
[30] W.J. McCarter, S. Garvin, Dependence of electrical impedance of cement-based materials on their moisture condition, J. Phys. D. Appl. Phys. 22 (1989) 1773–1776. doi:10.1088/0022-3727/22/11/033.
[31] D.E. Macphee, D.C. Sinclair, S.L. Cormack, Development of an Equivalent Circuit Model for Cement Pastes from Microstructural Considerations, J. Am. Ceram. Soc. 80 (1997) 2876–2884. doi:10.1111/j.1151-2916.1997.tb03206.x.
[32] G. Song, Equivalent circuit model for AC electrochemical impedance spectroscopy of concrete, Cem. Concr. Res. 30 (2000) 1723–1730. doi.org/10.1016/S0008-8846(00)00400-2.
[33] M. Cabeza, P. Merino, A. Miranda, X.R. Novoa, I. Sanchez, Impedance spectroscopy study of hardened Portland cement paste, Cem. Concr. Res. 32 (2002) 881–891. doi:10.1016/S0008-8846(02)00720-2
[34] B. Díaz, L. Freire, P. Merino, X.R. Nóvoa, M.C. Pérez, Impedance spectroscopy study of saturated mortar samples, Electrochim. Acta. 53 (2008) 7549–7555. doi:10.1016/j.electacta.2007.10.042.
[35] F. Leroux, J. Russias, C. Cau-dit-Coumes, F. Frizon, G. Renaudin, Low-to-Medium-Frequency AC Impedance Spectroscopy Investigations of Nanocrystalline Calcium Silicate Hydrate Dried Powders, J. Am. Ceram. Soc. 94 (2011) 2680–2687.doi: 10.1111/j.1551-2916.2011.04429.x.
[36] J.M. Ortega, I. Sánchez, M.A. Climent, Impedance spectroscopy study of the effect of environmental conditions in the microstructure development of OPC and slag cement mortars, Archives of civil and mechanical engineering 15 (2015) 569-583. doi:10.1016/j.acme.2014.06.002.
[37] J. Beaudoin, B. Tamtsia, Effect of drying methods on microstructural changes in hardened cement paste: an AC impedance spectroscopy evaluation, J. Adv. Concr. (2004). doi: 10.3151/JACT.2.113.
[38] W.J. McCarter, H.M. Taha, B. Suryanto, G. Starrs, Two-point concrete resistivity measurements: interfacial phenomena at the electrode–concrete contact zone, Meas. Sci. Technol. 26 (2015) 085007. doi:10.1088/0957-0233/26/8/085007.
[39] I.C. Fita, J.M. Cruz, C. Calvo, L. Soriano, J. Payá, I. Sánchez, Drying-rewetting cycles in ordinary Portland cement mortars investigated by electrical impedance spectroscopy, Constr. Build. Mater. 187 (2018) 954–963. doi:10.1016/J.CONBUILDMAT.2018.07.227.
[40] Y. Tan, H. Yu, W. Bi, N. Wang, N. Zhang, Hydration Behavior of Magnesium Oxysulfate Cement with Fly Ash via Electrochemical Impedance Spectroscopy, J. Mater. Civ. Eng. 31 (2019) 04019237. doi:10.1061/(asce)mt.1943-5533.0002827.
[41] J. Zhang, B. Dong, S. Hong, X. Teng, G. Li, W. Li, L. Tang, F. Xing, Investigating the influence of fly ash on the hydration behavior of cement using an electrochemical method, Constr. Build. Mater. 222 (2019) 41–48. doi:10.1016/J.CONBUILDMAT.2019.06.046.
[42] D.P. Almond, B. Vainas, The dielectric properties of random R - C networks as an explanation of

the `universal' power law dielectric response of solids, J. Phys. Condens. Matter. 11 (1999) 9081–9093. doi:10.1088/0953-8984/11/46/310.
[43] D.P. Almond, C.R. Bowen, Anomalous power law dispersions in ac conductivity and permittivity shown to be characteristics of microstructural electrical networks, Phys. Rev. Lett. 92 (2004) 157601. doi:10.1103/PhysRevLett.92.157601.
[44] R.F. Hamou, J.R. MacDonald, E. Tuncer, Dispersive dielectric and conductive effects in 2D resistor-capacitor networks, J. Phys. Condens. Matter. 21 (2009) 025904. doi:10.1088/0953-8984/21/2/025904.
[45] J.R. Macdonald, L.D. Potter, A flexible procedure for analyzing impedance spectroscopy results: Description and illustrations, Solid State Ionics. 24 (1987) 61–79. doi:10.1016/0167-2738(87)90068-3.
[46] J.R. Macdonald, Comparison of Parametric and Nonparametric Methods for the Analysis and Inversion of Immittance Data: Critique of Earlier Work, J. Comput. Phys. 157 (2000) 280–301. doi:http://dx.doi.org/10.1006/jcph.1999.6378.
[47] G.A. Niklasson, A fractal description of the dielectric response of disordered materials, J. Phys. Condens. Matter. 5 (1993) 4233–4242. doi:10.1088/0953-8984/5/25/013.
[48] A. Berg, G.A. Niklasson, K. Brantervik, B. Hedberg, L.-O. Nilsson, Dielectric properties of cement mortar as a function of water content, J. Appl. Phys. 71 (1992) 5897–5903.doi: 10.1063/1.350488.
[49] S.S. Yoon, H.C. Kim, R.M. Hill, The dielectric response of hydrating porous cement paste, J. Phys. D. Appl. Phys. 29 (1996) 869.doi: 10.1088/0022-3727/29/3/054.
[50] B.A. Boukamp, A Nonlinear Least Squares Fit procedure for analysis of immittance data of electrochemical systems, Solid State Ionics. 20 (1986) 31–44. doi:10.1016/0167-2738(86)90031-7.
[51] AENOR, AENOR: Norma UNE-EN 196-1:2005, Http://Www.Aenor.Es/. (n.d.). http://www.aenor.es/aenor/normas/normas/fichanorma.asp?tipo=N&codigo=N0034791#.WyJjVaczaUk (accessed June 14, 2018).
[52] AENOR, AENOR: Norma UNE-EN 197-1:2011, Http://Www.Aenor.Es/. (n.d.). http://www.aenor.es/aenor/normas/normas/fichanorma.asp?tipo=N&codigo=N0048623#.WyJiG6czaUk (accessed June 14, 2018).
[53] B. Boukamp, D. Blank, High-precision impedance spectroscopy: a strategy demonstrated on PZT, IEEE Trans. Ultrason. Ferroelectr. Freq. Control. 58 (2011) 2521–2530. doi:10.1109/TUFFC.2011.2115.